Field Trial of FPGA-Based Real-Time Sensing Transceiver over 524 km of Live Aerial Fiber

Mikael Mazur(1), Dennis Wallberg(2), Lauren Dallachiesa(1), Erik Börjeson(3), Roland Ryf(1), Magnus Bergroth(2), Börje Josefsson (2) Nicolas K. Fontaine(1), Haoshuo Chen(1), David T. Neilson(1), Jochen Schröder(4), Per Larsson-Edefors(3) and Magnus Karlsson(4)

(1) Nokia Bell Labs, 600 Mountain Ave., Murray Hill, NJ 07974, USA
(2) Sunet, Tulegatan 11, Stockholm, Sweden
(3) Department of Computer Science and Engineering, Chalmers University of Technology, Gothenburg, Sweden
(4) Department of Microtechnology and Nanoscience, Chalmers University of Technology, Gothenburg, Sweden

mikael.mazur@nokia-bell-labs.com, magnus.karlsson@chalmers.se

Abstract: We perform fiber sensing over a 524 km live network using a real-time coherent transceiver prototype. Polarization and length changes from the link consisting exclusively of aerial fiber wound around high-voltage power cables are continuously monitored.

1. Introduction

Recently, there has been an increased focus on using the telecom grid for fiber sensing. Sensing using deployed telecom networks is often categorized into two parts: Environmental sensing of the surrounding environment, and direct sensing for network protection/integrity. Examples of environmental sensing include earth quake detection using submarine [1] and terrestrial fibers [2], monitoring of whale migration [3], and traffic monitoring [4]. Examples of network integrity sensing include site intrusion detection [5] and detection of patch panel movement [6]. However the two are often mutually dependent as fiber break prevention inherently relies on detecting changes in the surrounding fiber environment. Fiber sensing is typically performed using techniques such as distributed acoustic sensing (DAS) [5] or Raman-based temperature sensing [7]. Depending on the implementation, DAS can be co-propagated with data channels avoiding the need for dark fiber [8]. While DAS is a powerful established technique that enables distributed measurements, it requires a dedicated sensing unit and channel space. Alternatively, fiber sensing using information extracted from coherent digital signal processing (DSP) has been proposed. State-of-polarization (SOP)-based sensing has been demonstrated using both prototype [9] and commercial products [1] and phase sensing has been shown using real-time [10] and offline research prototypes [11]. However, to maximize the gain of transceiver-based sensing, a thorough understanding of how to extract environmental information from the DSP is needed. An example of this would be to preventively detect that an aerial fiber span is increasing in length, which could indicate that a pole is starting to tilt.

In this work, we use an FPGA-based coherent transceiver sensing prototype to perform fiber sensing over a 524-km loop-back link consisting exclusively of aerial fiber wrapped around high voltage power grid conductors. To the best of our knowledge, this is the first fiber sensing study using a coherent transceiver for these types of fibers. We focus on the use of the dynamic equalizer as a sensor, relying on fast 100µs readouts of the equalizer states built into the parallel and pipelined real-time DSP implementation. We first demonstrate how the DSP-based timing recovery module can be turned into a time-of-flight sensor, enabling continuous monitoring of the fiber length. We continuously monitor the length over a 70h period and show good quantitative agreement with temperature data from three weather stations present along the link. We then focus on polarization measurements and, using wind data, analyze the result and different wind conditions. We show how all environmental changes are obscured by strong polarization changes driven by 50 Hz changes induced by transmission fibers being wound around the power lines. Focusing on the sub-50Hz regime of environmental sensing interest, we show how the polarization state varies depending on wind conditions. Our results show how continuous fiber sensing using coherent transceivers over aerial fibers can aid with network integrity and enable secondary use cases of an already existing communication infrastructure for environmental sensing and infrastructure monitoring.

2. Experimental Setup

The experimental setup is shown in Fig. 1(a). The FPGA-based prototype transceiver was connected to Sunet's (Swedish University Network's) live fiber network at the ROADM node in Gothenburg, Sweden. Multiple live coherent transceivers were also connected through the same wavelength selective switch (WSS). A map of Sunet's network is shown in Fig. 1(b) with a zoom-in shown in Fig. 1(c). The route used is highlighted in red and consisted exclusively of aerial fiber. The fiber is mounted along the high voltage power lines, making it very exposed to environmental variations. Throughout the link, 5 ROADM nodes were passed before reaching Karlstad. Three weather stations belonging to the Swedish Meteorological and Hydrological Institute (SMHI) were present along the approximate route of the fiber, as shown by the orange and green dots in Fig. 1(c). The orange dots denote stations monitoring both temperature and wind while the green represents temperature only. The sampling rate of 1h. In case of wind, the measurement reported was the maximum wind speed per hour.

A detailed sketch of the transceiver prototype is shown in Fig. 1(d). An FPGA with integrated digital-to-analog (DACs) and analog-to-digital (ADCs) (Xilinx ZU48DR) was used to implement the real-time transceiver module.

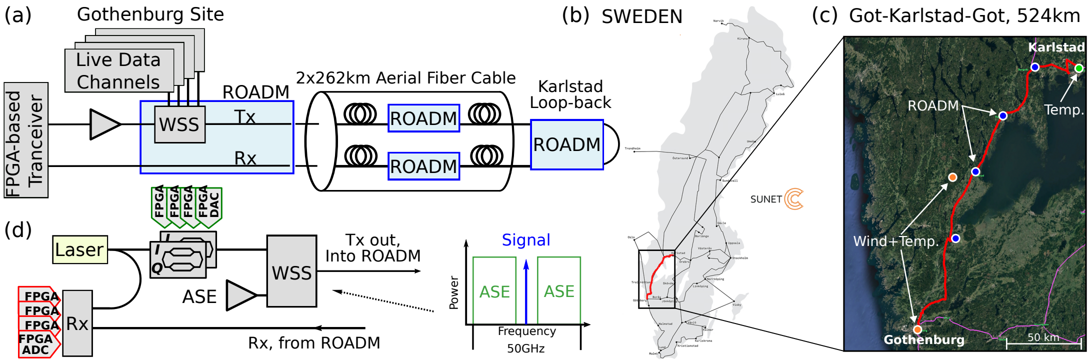

Fig. 1: (a) Experimental setup showing the connection of our real-time transceiver prototype to the live network. The low baud-rate signal was combined with ASE loading and connected to the live ROADM with a 50 GHz allocated channel bandwidth. (b) A map of Sunet's Swedish fiber network with the 524 km route from Gothenburg to Karlstad and back highlighted in red. The route passed five ROADM nodes. (c) Zoom-in of the route with weather stations present. Orange denotes a station measuring both wind and temperature, green denotes temperature and blue respresents a ROADM node. (d) Detailed sketch of the FPGA-based transceiver prototype. The 50 GHz channel was generated by combining the signal with ASE in a WSS with 6.25 GHz addressability and 1 wavelength slot devoted to the test signal and the remaining 43.75 GHz filled with ASE.

The digital transmitter operated with a parallelization degree of 16 at a clock rate of 125 MHz to generate a two-fold oversampled 1-GBd signal. The modulated signal was pilot-based with QPSK-based pilots and polarization-multiplexed 16-QAM payload. The real-time implementation used one lane pilots and 8-bit precision. The ADCs were connected via 4 differential RF amplifiers to a dual polarization IQ-modulator seeded by a regular telecom external cavity laser with ∼10-kHz linewidth. The signal was then combined with an amplified spontaneous emission (ASE) noise in a commercial WSS with 6.25-GHz resolution. This was needed to ensure that the prototype channel "looked" like a live channel, both in terms of launch power and bandwidth, which was necessary in order to create a proper channel plan to pass the five ROADMs along the link. The loop-back in Karlstad was implemented using the ROADM node, routing our channel back to Gothenburg where the drop node of the ROADM was used to extract the test signal. However, due to the lack of a second WSS, the full band was injected into the coherent receiver. After coherent detection, using a copy of the transmitter laser in a homodyne-like configuration, the signals were digitized using four ADCs operating at 2 GS/s with 8 bits of resolution. The real-time DSP consisted of front-end correction, equalization using a 17 T/2-spaced complex taps 2×2 multiple-input multiple-output (MIMO) equalizer in a butterfly configuration and carrier phase estimation using the principal component method [12]. In line with the transmitter, the receiver was running at a clock rate of 125 MHz using 8-bit word length. The equalizer coefficients used 9-bit precision and two additional bits were included in the error calculation. A cascade of first-in-first-outs (FIFOs) implemented using RAM were used to support full readout of the equalizer state at MHz rate. The data was then collected by an onboard CPU and uploaded to the cloud. To enable long-term measurements without overloading the internet connections, a sampling rate of 100 µs was selected.

3. Results and Conclusion

We first used the dynamic equalizer to perform time-of-flight (ToF) measurements over the aerial fiber link. If the fiber is expanding or contracting, the dynamic equalizer moves the temporal taps center of mass around to match the delay of the aerial fiber link. Note that in a non-loopback configuration, clock synchronization is necessary to separate clock drifts from fiber changes. Figure 2(a) shows the magnitude of 17 temporal taps for the 4 equalizer components, taken 1h apart. Here we can clearly see how the center of mass of the taps move around as the fiber changes. Figure 2(b) shows the unwrapped measurement over a time scale of approximately 70h. Here we can clearly see how the fiber stretches and contracts during different times of the day. Figure 2(b) also shows the average temperature over the 3 measurement stations shown in Fig. 1(c). Good quantitative agreement is found between the two. Using typical thermal sensitivity of single-mode fiber of 40 ps/degK/km, we expect around 80 ns change for a temperature change of 4 degrees. While this is in line with the measurements in Figure 2(b), it is worth noting that in the long multi-span link, uncertainty in the thermal sensitivity of the cable, sparse temperature measurements and thermal dissipation from the electrical conductor naturally all contribute to deviations. Still a solid agreement is found, and accuracy could be improved by applying this technique on a span-by-span basis using for example dedicated monitoring channels. The wind recording, averaged between the two measurement stations from Fig. 1(c), is shown in Fig. 2(c). The two points selected correspond to the highest and lowest wind conditions observed over our measurement time window. Figure 2(d) shows the Poincare sphere for a 1 second measurement of the SOP at the lowest wind speed condition. Here we can clearly see the SOP response is dominated by a fast rotation around a single axis, which we believe is from the Farady effect induced by the current in the power cable. Monitoring of both frequency deviations and length changes, normally done using dedicated

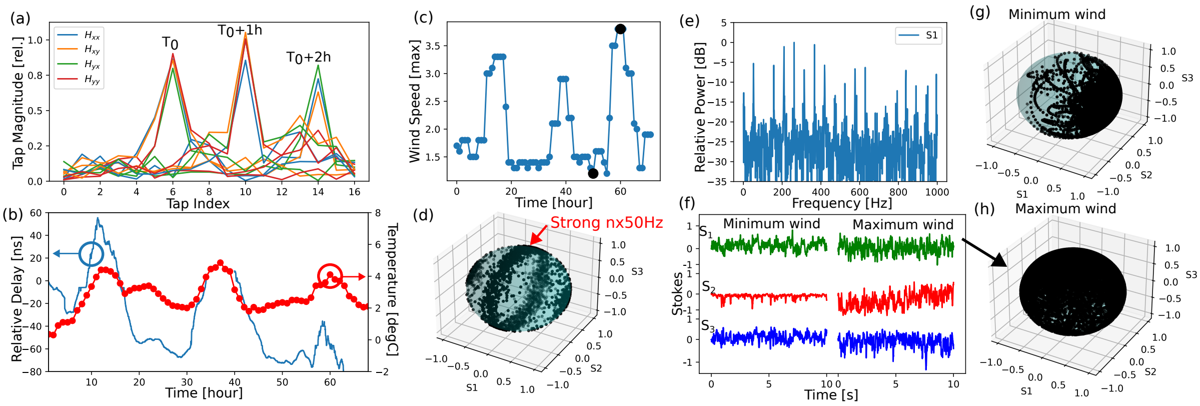

Fig. 2: (a) Magnitude of equalizer taps taken at time instances 1h apart. The change in temporal position can be translated into a stretch/contraction of the fiber link. (b) Using this effect for time-of-flight measurements over 524 km of aerial fiber. The temperature shown is the average temperature of the 3 measurement stations shown in Fig. 1. (c) Average wind speed in m/s. (d) Poincaré representation of the SOP change during 10 seconds at of minimum wind speed. (e) Corresponding Fourier transform of S1 showing the strong presence of 50 Hz and overtones. The fiber is wound around the high voltage conductor. (g) and (h) Poincaré representation of polarization rotations after applying a 45 Hz low-pass filter for low and high wind, respectively.

power line sensing systems, is also essential for power grid monitoring and maintenance [13]. The corresponding Fourier transform for S1 is shown in Figure 2(e), highlighting the strong presence of 50 Hz and its harmonics. This is in line with previous direct SOP measurements of fiber hanging from power lines [14] and differs significantly from SOP changes in buried cables [15]. In addition, the winding of the power cable around the conductor is expected to increase the Faraday effect linearly with number of wraps. Operating a loopback through the same cable, assuming that the magnetic field is stable over the round-trip propagation time, furthermore doubles the induced rotation [16]. This strong dependence, and large presence of fibers along power lines show how regular coherent transceivers can be used to performed detailed monitoring of the AC-current's magnitude and frequency via SOP measurements. Given that environmental perturbations from wind is in the sub-10Hz, these harmonics naturally mask their presence. However, after filtering out all frequencies beyond 45 Hz, the resulting Stokes movement is shown in Fig. 2(g) and (h) for the case of minimum and maximum wind, respectively. Figure 2(f) shows the separated Stokes measurements. From the Poincaré representation we clearly observe a large difference, indicating that the link is strongly susceptible to wind-induced polarization changes.

In conclusion, we have demonstrated fiber sensing using a real-time FPGA-based coherent transceiver prototype over 524 km of aerial fiber spun around power lines. We demonstrated fiber length sensing using time-of-flight measurement extracted from the real-time equalizer implementation and correlated the measurements with temperature from measurement stations along the link. We furthermore analyzed the state-of-polarization, showing a strong present of n·50 Hz oscillations likely from the Faraday effect induced by the spun fiber. By filtering out the low-frequency part, we also analyzed the polarization stability in the case of various wind conditions. Our results show the potential for coherent transceivers to perform continuous sensing over aerial fibers, enabling both new use cases via environmental and/or current sensing and improving the network integrity by continuously monitoring the health of the fiber link.

References

1. Z. Zhan *et al*, "Optical polarization–based seismic and water sensing on transoceanic cables", Science, 371, (6532), 2021.
2. H. Martins *et al*, "Monitoring of remote seismic events in metropolitan area ibers using distributed...", Proc. OFC paper M2J.1, 2019.
3. M. Landrø *et al*, "Sensing whales, storms, ships and earthquakes using an Arctic fibre-optic cable", ESSOA, 29 2021.
4. G. A. Wellbrock *et al*, "Field trial of vibration detection and localization using Operational Telecom...", Proc. OFC paper F3B.2, 2021.
5. E. Ip *et al*, "Distributed fiber sensor network using telecom cables as sensing media: technology advancements...", JOCN, 14 (1) 2022.
6. M. Mazur *et al*, "Continuous Fiber Sensing Over Field-Deployed Metro Link Using Real-Time...", Proc. ECOC paper Mo4A.2, 2022.
7. J. P. Dakin *et al*, "Distributed optical fibre Raman temperature sensor using a semiconductor...", Elec. Lett. 21 (13), 1985.
8. S. Guerrier *et al*, "Vibration Detection and Localization in Buried Fiber Cable after 80km of SSMF...", Proc. OFC paper M2F.3, 2022.
9. F. Boitier *et al*., "Proactive Fiber Damage Detection in Real-time Coherent Receiver", Proc. ECOC, paper Th.2.F.1 (2017)
10. M. Mazur *et al*, "Transoceanic Phase and Polarization Fiber Sensing Using Real-Time Coherent..., Proc. OFC paper M2F.2, 2022.
11. E. Ip *et al*, "Vibration Detection and Localization Using Modified Digital Coherent Telecom Transponders", JLT, 40 (5) 2022.
12. E. Börjeson and P. Larsson-Edefors, "Energy-efficient implementation of carrier phase recovery for...", JLT, 39 (2). 2021.
13. Y. Yang *et al*, "Power line sensornet - a new concept for power grid monitoring", IEEE Pow. Eng. Meeting, 2006.
14. J. Wuttke *et al*, "Polarization Oscillations in Aerial Fiber Caused by Wind and Power-Line Current", PTL 15(26), 2003.
15. M. Karlsson *et al*, "Long-term measurement of PMD and polarization drift in installed fibers", JLT, 18 (7),. 2000.
16. L. Palmieri *et al*, "Distributed measurement of high electric current by means of polarimetric optical fiber sensor", JLT, 23 (9), 2015.